

## Nature and properties of the Johari–Goldstein $\beta$ -relaxation in the equilibrium liquid state of a class of glass-formers

K. L. Ngai, Peter Lunkenheimer, C. León, Ulrich Schneider, Robert Brand, Alois Loidl

### Angaben zur Veröffentlichung / Publication details:

Ngai, K. L., Peter Lunkenheimer, C. León, Ulrich Schneider, Robert Brand, and Alois Loidl. 2001. "Nature and properties of the Johari–Goldstein  $\beta$ -relaxation in the equilibrium liquid state of a class of glass-formers." *The Journal of Chemical Physics* 115 (3): 1405–13.  
<https://doi.org/10.1063/1.1381054>.



RESEARCH ARTICLE | JULY 15 2001

## Nature and properties of the Johari–Goldstein $\beta$ -relaxation in the equilibrium liquid state of a class of glass-formers


K. L. Ngai; P. Lunkenheimer; C. León; U. Schneider; R. Brand; A. Loidl




*J. Chem. Phys.* 115, 1405–1413 (2001)

<https://doi.org/10.1063/1.1381054>






Lock-in Amplifier



Boxcar Averager



Zurich  
Instruments

Boost Your Optics and  
Photonics Measurements

Find out more

# Nature and properties of the Johari–Goldstein $\beta$ -relaxation in the equilibrium liquid state of a class of glass-formers

K. L. Ngai

*Naval Research Laboratory, Washington, D.C. 20375-5320*

P. Lunkenheimer

*Experimentalphysik V, Institut für Physik, Universität Augsburg, D-86135 Augsburg, Germany*

C. León

*GFMC, Dpto. Física Aplicada III, Facultad de Ciencias Físicas, Universidad Complutense de Madrid, E-28040 Madrid, Spain*

U. Schneider,<sup>a)</sup> R. Brand,<sup>b)</sup> and A. Loidl

*Experimentalphysik V, Institut für Physik, Universität Augsburg, D-86135 Augsburg, Germany*

(Received 22 February 2001; accepted 2 May 2001)

Previous dielectric relaxation measurements of glycerol and propylene carbonate and new results on propylene glycol performed below the conventional glass transition temperatures  $T_g$  after long periods of aging all show that the excess wing (a second power law at higher frequencies) in the isothermal dielectric loss spectrum, develops into a shoulder. These results suggest that the excess wing, a characteristic feature of a variety of glass-formers, is the high frequency flank of a Johari–Goldstein  $\beta$ -relaxation loss peak submerged under the  $\alpha$ -relaxation loss peak. With this interpretation of the excess wing assured, the dielectric spectra of all three glass-formers measured at temperatures above  $T_g$  are analyzed as a sum of a  $\alpha$ -relaxation modeled by the Fourier transform of a Kohlrausch–Williams–Watts function and a  $\beta$ -relaxation modeled by a Cole–Cole function. Good fits to the experimental data have been achieved. In addition to the newly resolved  $\beta$ -relaxation on propylene glycol, the important results of this work are the properties of the  $\beta$ -relaxation in this class of glass-formers in the equilibrium liquid state obtained over broad frequency and temperature ranges. © 2001 American Institute of Physics.

[DOI: 10.1063/1.1381054]

## I. INTRODUCTION

The glass transition can be considered as one of the great unresolved problems in solid state physics. In recent years, the interest has focused on the investigation of the molecular dynamics of glass-forming liquids, which is governed by a wealth of different processes, many of them not completely understood until now. Mainly due to the broad dynamic range accessible, dielectric spectroscopy has proven an ideal tool to study these processes. Dielectric loss spectra of glass-forming materials are dominated by the  $\alpha$ -peak. It is contributed by the structural relaxation, which is dramatically slowed down when the glass-temperature is approached. In the supercooled state, its spectral shape deviates from the monodispersive Debye form and significantly broadens with decreasing temperature. In addition, the corresponding  $\alpha$ -relaxation time  $\tau_\alpha$  shows pronounced deviations from thermally activated Arrhenius behavior.

At frequencies some decades above the  $\alpha$ -peak frequency  $\nu_p$ , in a class of glass-formers an excess contribution to the high-frequency flank of the  $\alpha$ -peak shows up.<sup>1–4</sup> It can be described formally as a second power law,  $\epsilon'' \sim \nu^{-b}$ , following the  $\nu^{-\beta}$  power law found at  $\nu > \nu_p$ .<sup>2,3</sup> Nagel and co-

workers found that by an appropriate scaling of the axes, it is possible to collapse the  $\epsilon''(\nu)$ -curves, including the peak and excess wing, for different temperatures and even for different materials onto one master curve.<sup>1</sup> These authors suggested the peak and the excess wing are inseparable parts of one and the same  $\alpha$ -relaxation, which, when scaled, is represented by the master curve. Consistent with this suggestion, theoretical models including the dynamically correlated domains<sup>5</sup> of Chamberlin and the frustration-limited-domains of Tarjus and Kivelson<sup>6</sup> have been proposed as explanations of this peculiar shape of the  $\alpha$ -relaxation. Until now, there is no commonly accepted microscopic explanation for the occurrence of the excess wing and its intriguing scaling properties.

In many other glass-forming materials, besides the  $\alpha$ -peak, there is clear evidence of the presence of a higher frequency relaxation process, commonly called the  $\beta$ -relaxation, because it gives rise to an additional peak or shoulder in  $\epsilon''(\nu)$ . Already three decades ago, Johari and Goldstein systematically investigated such relaxations in supercooled liquids without intramolecular degrees of freedom.<sup>7</sup> Based on these results, it was proposed that the occurrence of these so-called Johari–Goldstein (J–G)  $\beta$ -relaxations is an inherent property of the supercooled state.<sup>7,8</sup> However, the microscopic origin of these  $\beta$ -relaxations is still a matter of controversy (see, e.g., Ref. 4). The  $\alpha$  and  $\beta$  relaxation times often show a tendency to

<sup>a)</sup>Present address: Heraeus Quarzglas, Fiber Optic Division, Research and Development, Quarzstrasse, D-63450 Hanau, Germany.

<sup>b)</sup>Present address: Vacuumschmelze GmbH, HT-E M, Grüner Weg 37, D-63450 Hanau, Germany.

merge at high temperatures, and the  $\beta$ -relaxation time  $\tau_\beta(T)$  is often reported or believed to have thermally activated Arrhenius temperature dependence. The Arrhenius behavior of  $\tau_\beta(T)$  seems well established below the vitrification temperature  $T_g$ . However, above  $T_g$  the situation is not clear. For most glass-formers, in which the J–G  $\beta$ -relaxation is observed, the  $\beta$ -relaxation frequency at  $T_g$ ,  $\nu_\beta(T_g)$  is already quite high. There are only a few decades of frequency above  $\nu_\beta(T_g)$  before the  $\beta$ -relaxation merges with the  $\alpha$ -relaxation. In this region, the  $\beta$ -relaxation gains strength with increasing temperature, making an unambiguous separation of the two relaxation processes difficult. These problems contribute to the uncertainty in the temperature dependence of  $\tau_\beta(T)$  at temperatures above  $T_g$ .

Until recently, it was commonly assumed that excess wing and  $\beta$ -relaxations are due to different microscopic processes. It was proposed that there are two classes of glass formers: “Class A” without a  $\beta$ -process, but showing an excess wing, and “Class B” with a  $\beta$ -process.<sup>4,9,10</sup> However, there are also treatments and explanations of both classes on the same footing.<sup>2,11–15</sup> Indeed recently, from dielectric experiments performed below the glass temperature  $T_g$ , after long aging times, strong indications were obtained that the excess wing is simply the high-frequency flank of a  $\beta$ -peak, submerged under the dominating  $\alpha$ -peak.<sup>16</sup> These low-temperature measurements were motivated by the well-established fact that the  $\alpha$ - and  $\beta$ -peak frequencies separate progressively when the temperature is lowered. After aging times of up to five weeks to reach thermodynamic equilibrium at sub- $T_g$  temperatures, the power-law excess wing was observed to develop into a shoulder, giving strong hints for a  $\beta$ -relaxation as origin of the excess wing. Furthermore, as discussed in detail in Ref. 16, some evidence for this notion can also be found in earlier literature.<sup>2,15,17–23</sup> In the framework of this picture, the above-mentioned two classes of glass-formers may be distinguished by just a different temperature evolution of the  $\beta$ -dynamics: In Class B materials,  $\tau_\beta(T)$  has a much weaker temperature dependence than  $\tau_\alpha(T)$ , leading to a clear separation of  $\alpha$ - and  $\beta$ -peak at low temperatures. By contrast, in Class A materials,  $\tau_\beta$  may track along  $\tau_\alpha$  more closely at all temperatures above  $T_g$  and only the high-frequency flank of the  $\beta$ -peak or the excess wing is visible.

In this context, it shall be mentioned that the above scenario is consistent with the recently found correlation of  $\tau_\beta(T_g)$  and the value of the Kohlrausch-exponent,  $(1-n)$ , also at  $T_g$ ,<sup>24</sup> of the Kohlrausch–Williams–Watts (KWW) function,<sup>25</sup>

$$\phi(t) = \exp[-(t/\tau_\alpha)^{1-n}]. \quad (1)$$

Here  $(1-n)$  is the KWW exponent, which is usually denoted by  $\beta_{\text{KWW}}$ . The one-sided Fourier transform of the KWW function offers one way to fit the dielectric  $\alpha$ -loss peak. Glass-formers without a well-resolved  $\beta$ -relaxation (Class A) have a relatively narrower  $\alpha$ -peak and larger  $[1-n(T_g)]$ , which, by virtue of this correlation, implies closer proximity of  $\tau_\alpha$  and  $\tau_\beta$ . Consequently, the broad  $\beta$ -peak becomes submerged under the  $\alpha$ -peak and cannot be resolved. An explanation of this correlation has been given

within the framework of the coupling model.<sup>26,27</sup> In the coupling model, there is a primitive relaxation process, which like the J–G  $\beta$ -relaxation, is devoid of intermolecular coupling. Therefore, the primitive relaxation time,  $\tau_o$ , and the  $\beta$ -relaxation time,  $\tau_\beta$ , are expected to be comparable, i.e.,

$$\tau_o \approx \tau_\beta. \quad (2)$$

In the coupling model,  $n$  in Eq. (1) is called the coupling parameter and  $\tau_o$  is related to  $\tau_\alpha$  by

$$\tau_o = (t_c)^n (\tau_\alpha)^{1-n}. \quad (3)$$

Here  $t_c$  in Eq. (3) is the crossover time from primitive relaxation to cooperative relaxation and has the approximate value of  $2 \times 10^{-12}$  s for small molecular liquids.<sup>28</sup> The separation between  $\tau_\alpha$  and  $\tau_o$  from Eq. (3) is given by

$$\log \tau_\alpha - \log \tau_o = n \log \tau_\alpha - n \log t_c, \quad (4)$$

which decreases as  $n$  becomes smaller, and vanishes when  $n$  is exactly equal to zero. From Eq. (2), the same can be said on the separation between  $\tau_\alpha$  and  $\tau_\beta$ , i.e.,

$$\log \tau_\alpha - \log \tau_\beta \approx n \log \tau_\alpha - n \log t_c. \quad (5)$$

Also, the Nagel-scaling may be explained in this way as was shown in Ref. 13.

In the present work, we analyze dielectric spectra of three low-molecular-weight glass-formers that are known to reveal well-pronounced excess wings: Glycerol ( $T_g \approx 185$  K), propylene carbonate (PC,  $T_g \approx 159$  K), and propylene glycol (PG,  $T_g = 168$  K). The presented loss spectra of glycerol and PC have been previously published in Refs. 16–18, 29, and 30. The results for glass-forming PG, including aging experiments similar to those performed in glycerol and PC,<sup>16</sup> are new. One aim of the present work is to demonstrate that for all materials investigated, the spectra below and above  $T_g$  can be consistently described by a superposition of an  $\alpha$ - and  $\beta$ -peak. In addition, information on the properties of the  $\beta$ -relaxation shall be obtained, especially concerning the temperature development of its relaxation time, width parameter and amplitude. Finally, the results are compared to the predictions within the above-mentioned scenario, assuming that the J–G  $\beta$ -relaxation is closely related to the primitive  $\alpha$ -relaxation of the coupling model.

## II. EXPERIMENTAL DETAILS

To collect dielectric data in a broad frequency range, various experimental setups were used, including time domain spectrometers ( $10 \mu\text{Hz} \leq \nu \leq 1$  kHz), frequency response analyzers and LCR-meters ( $10 \mu\text{Hz} \leq \nu \leq 30$  MHz), impedance analyzers (reflectometric technique,  $1 \text{ MHz} \leq \nu \leq 1.8$  GHz), a network analyzer (reflection and transmission,  $100 \text{ MHz} \leq \nu \leq 30$  GHz), a quasi-optic submillimeter wavelength spectrometer (transmission and phase measurement,  $40 \text{ GHz} \leq \nu \leq 1.2$  THz), and a Fourier-transform infrared spectrometer (transmission,  $600 \text{ GHz} \leq \nu \leq 3$  THz). For more experimental details on the measurements above  $T_g$ , the reader is referred to Refs. 29 and 31.

For the high-precision measurements below  $T_g$ , which are of special interest in the context of the present paper, a Novocontrol alpha analyzer was used, covering a frequency

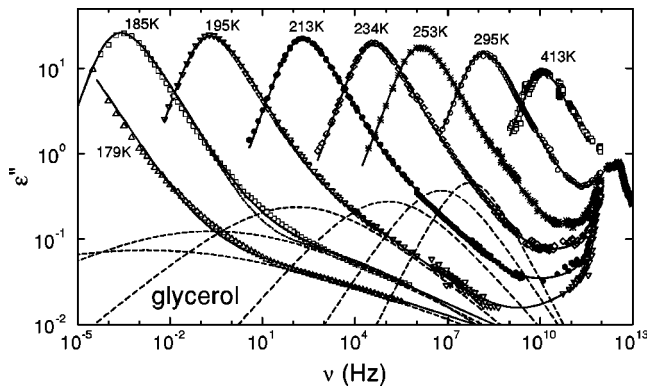


FIG. 1. Frequency-dependent dielectric loss of glycerol for various temperatures (to maintain readability only a selection of temperatures is shown) (Refs. 16,17,29,30,32). The curve at 179 K was obtained after aging for five weeks, ensuring that thermodynamic equilibrium was reached (Ref. 16). The solid lines are fits with the sum of a KWW function, a CC function and the terms  $\epsilon_c + c_3 \nu^{0.3} + c_n \nu^n$  (see text). For  $T \geq 295$  K, the CC function was omitted as, here,  $\alpha$ -peak and excess wing have completely merged. The broad peaks at the bottom (dashed lines) show the CC-curves for the  $\beta$ -relaxation used to explain the data in the excess wing region. The dashed-dotted line shows a fit of the 185 K curve with  $\tau_\beta$  fixed at the primitive relaxation time of the coupling model  $\tau_o$ .

range of  $10 \mu\text{Hz} \leq \nu \leq 1 \text{ MHz}$ .<sup>16</sup> This frequency response analyzer allows for the detection of values of  $\tan \delta$  as low as  $10^{-4}$ . For the measurements, parallel plane capacitors having an empty capacitance up to 100 pF were used. To keep the samples at constant temperature for up to five weeks during aging, a closed-cycle refrigerator system was used. The samples were cooled from a temperature 20 K above  $T_g$ , with the maximum possible cooling rate of about 3 K/min. The final temperature was reached without temperature undershoot. For zero point of the aging times reported below, we took the time when the desired temperature was reached, about 200 s after passing  $T_g$ . The temperature was kept stable within 0.02 K during the complete aging time.

### III. RESULTS AND DISCUSSION

#### A. Excess wing and the $\beta$ -relaxation identified

Figures 1, 2, and 3 show the dielectric loss spectra of glycerol,<sup>16,17,29,30,32</sup> PC,<sup>16,18,29,30,32</sup> and PG, respectively, for selected temperatures. The results for glycerol and PC cover an exceptionally broad frequency range of more than 17 decades. All spectra are dominated by the  $\alpha$ -peak shifting through the frequency window with temperature. For glycerol and PC (Figs. 1 and 2), in the microwave and infrared region, a minimum of  $\epsilon''(\nu)$  is followed by another peak at about 1 THz, often called the “boson peak.” These features are not within the scope of the present work. Detailed discussions of the high-frequency results using different approaches can be found in Refs. 18, 19, 30, 33–35.

For low temperatures, approaching  $T_g$ , the  $\alpha$ -peak reveals a well-pronounced excess wing. In Ref. 16, it was shown for glycerol and PC that at  $T < T_g$ , the excess wing develops into a shoulder during aging. In Figs. 1 and 2, for  $T < T_g$ , data measured in full thermodynamic equilibrium are shown, obtained after the maximum aging time of about five weeks.<sup>16</sup> For PC at 152 K and (somewhat difficult to

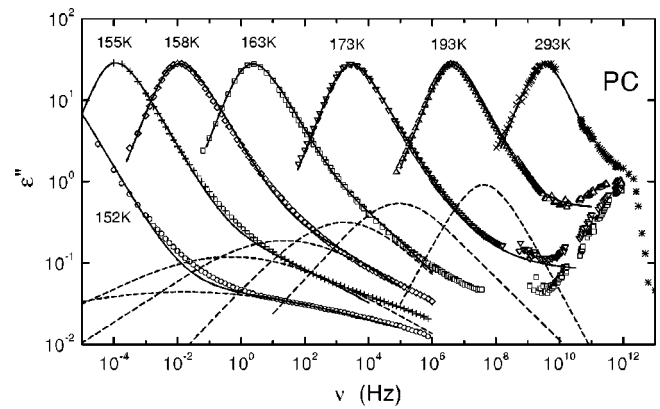


FIG. 2. Frequency-dependent dielectric loss of PC for various temperatures (to maintain readability only a selection of temperatures is shown) (Refs. 16,18,29,30). The curves at  $T < T_g$  were measured after suitable aging times to ensure thermodynamic equilibrium was reached (Ref. 16). The solid lines at  $T \leq 193$  K are fits of the  $\alpha$ -peak and excess-wing region with the sum of a KWW function and a CC function, with  $\tau_\beta$  fixed at the primitive relaxation time of the coupling model  $\tau_o$  at all temperatures. At high temperatures, where a minimum is observed, an additional constant loss term is included in the fit. At 293 K only a KWW fit is shown. The broad peaks at the bottom (dashed lines) show the CC-curves for the  $\beta$ -relaxation used to explain the data in the excess wing region. The CC peak frequency and peak height increase monotonically with temperature and this order can be used to identify which CC-curve is associated with which isothermal data set.

resolve in the chosen scale) for glycerol at 179 K, a shoulder (i.e., a negative curvature) is observed in the excess wing region, indicating the presence of a  $\beta$ -relaxation peak. In the inset of Fig. 3, we present new results from aging measurements performed at 157 K in glass-forming PG. The aging times range from 300 s to 6.5 days. The frequency window mainly covers the excess wing region. The somewhat steeper increase of  $\epsilon''(\nu)$  towards the lowest frequencies is contributed by the  $\alpha$ -relaxation, whose peak lies outside the experimental frequency window. Similar to the results of glycerol and PC in Ref. 16, a shoulder clearly shows up for the long-

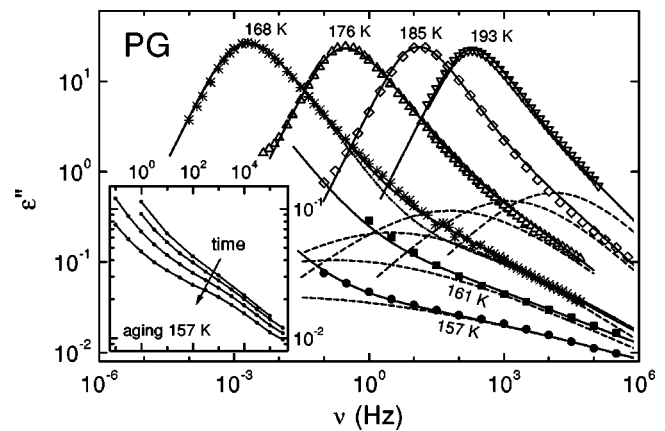


FIG. 3. Frequency dependent dielectric loss of PG for various temperatures (to maintain readability only a selection of temperatures is shown). The curve at 161 K was measured in thermodynamic equilibrium after aging for 53 min. The 157 K curve was measured after aging for 6.5 d, which was not sufficient to reach thermodynamic equilibrium. The solid, dashed and dashed-dotted lines have the same meaning as in Fig. 1. The inset shows the dielectric loss at 157 K for selected aging times (from top to bottom  $\log_{10}[t(s)] = 2.5, 3.5, 4.5, 5.75$ ).

est aging times. For the explanation of the observed aging behavior, we follow the arguments already laid out in Ref. 16: When cooled below  $T_g$ , glass-forming materials fall out of thermodynamic equilibrium. Keeping the samples at a constant temperature below  $T_g$  for extended times (“aging”), thermodynamic equilibrium is continuously being recovered. During aging, the  $\alpha$ -peak progressively shifts to lower frequencies due to a continuous decrease of the fictive temperature<sup>36</sup> towards the “true” temperature. In the inset of Fig. 3, this leads to the observed stronger time-dependent decrease at low frequencies, although the  $\alpha$ -peak itself, being located outside of the covered frequency window, cannot be seen. As the  $\beta$ -peak, causing the excess wing, is less affected by aging, both peaks become successively separated with increasing aging time and the  $\beta$ -peak finally shows up in the form of the observed shoulder. These results in PG give further evidence that, generally, the excess wing results from a  $\beta$ -relaxation peak submerged under the dominating  $\alpha$ -peak. It should be mentioned that in the present experiments carried out with a maximum aging time of 6.5 days, thermodynamic equilibrium was not reached. This can be deduced from the time-dependence of  $\varepsilon''(\nu)$ , which has not shown saturation for  $t \leq 6.5$  days.<sup>37</sup> However, this fact does not affect the validity of the above conclusions. The Nagel scaling<sup>1</sup> of the excess wing as well as theories<sup>5,6</sup> proposed to explain its appearance have considered the excess wing as an integral part of the  $\alpha$ -relaxation and not a separate J–G relaxation. The scaling proposal and these theories continue to predict the excess wing but not its development to become a shoulder. Hence, these theories, in their present forms, are in conflict with the aging data. However, it shall be mentioned that a recent extension of the Weiss mean-field theory for finite systems, using the model of dynamically correlated domains,<sup>5</sup> seems to be able to explain the present spectra, including the excess wing.<sup>38</sup> Interestingly, within this framework the occurrence of an excess wing is attributed to a superposition of peaks or shoulders, which are present in addition to the  $\alpha$ -peak, in good accord with the scenario developed above.

In the following, the spectra will be analyzed assuming a simple additive superposition of the  $\alpha$ - and the  $\beta$ -peak. The spectral shape of the  $\alpha$ -peak is often described employing the Fourier transform of the KWW function [see Eq. (1)].<sup>25</sup> This originally and purely phenomenological function has been theoretically derived in a variety of models<sup>27,39</sup> and is also used in the coupling model for the description of the  $\alpha$ -relaxation at  $t > t_c$ .<sup>27,28</sup> For glycerol and PC, it was shown, e.g., in Refs. 16 and 17, that the empirical Cole–Davidson (CD) function<sup>40</sup> leads to somewhat better fits of the  $\alpha$ -peak. However, in order to compare the results to the predictions of the coupling model, the KWW function is used in the present work. In materials showing clear  $\beta$ -peaks (Class B), their spectral shape can often be described by the empirical Cole–Cole (CC) function,<sup>41</sup>

$$\varepsilon_{\beta}^*(\nu) = \frac{\Delta\varepsilon_{\beta}}{1 + (i2\pi\nu\tau_{\beta})^{\gamma}}. \quad (6)$$

Here  $\Delta\varepsilon_{\beta}$  is the dielectric strength of the  $\beta$ -peak and  $\gamma$  de-

termines its width. Consequently, in order to describe  $\alpha$ -peak and excess wing in Figs. 1–3, we used a sum of a one-sided Fourier transform of a KWW and a CC function. Similar analyses were performed in Refs. 2, 12–14, and 30. The results of fits with this ansatz are shown in Figs. 1–3 as solid lines. For all materials, a satisfactory agreement of experimental data and fits for both, temperatures above and below  $T_g$ , can be stated.<sup>42</sup> In order to demonstrate that the high-frequency contributions in glycerol and PC, mentioned above, do not influence the quality of the fits, for glycerol, the shallow minimum and the increase at high frequencies towards the boson peak were also taken into account. A microscopic description of the minimum in glycerol at high temperatures is provided by the mode coupling theory of the glass transition,<sup>43</sup> as was shown in Refs. 29, 30 and 33. For the present purpose, the terms  $\varepsilon_c + c_3\nu^{0.3} + c_n\nu^n$  were used.<sup>30,35</sup> Adding these phenomenological terms, which leads to a satisfactory fit of the minimum at all temperatures, does not diminish the good description of the excess wing by a  $\beta$ -relaxation (Fig. 1).

The dashed lines show the underlying  $\beta$ -peaks as resulting from the fits. It should be noted that, especially at high temperatures, the parameters of the  $\beta$ -relaxation are partly correlated and, therefore, have rather large uncertainties. Therefore, in this region, parts of the parameters were fixed to avoid unreasonable jumps in their temperature developments. Nevertheless, overall these results clearly demonstrate that the experimental spectra of typical Class A glass-formers, including the power-law excess-wings at  $T > T_g$  and the shoulders at  $T < T_g$  (after aging), can be well-described by the superposition of the  $\alpha$ -peak and a  $\beta$ -peak that lies in its immediate vicinity. This description also indicates that the excess wing observed is actually a part of the  $\beta$ -relaxation, whenever it cannot be resolved either as a shoulder or peak.

The fits to the spectra of glycerol and PG in Figs. 1 and 3 are done by varying the parameters of the  $\beta$ -relaxation,  $\Delta\varepsilon_{\beta}$ ,  $\gamma$  and  $\tau_{\beta}$ . A similar procedure has been applied to PC with results (not shown here) that fit the data as well as shown for glycerol and propylene glycol. A variation of the procedure is applied to PC in the fits given in Fig. 2. The fits to the PC data are performed at each temperature by fixing  $\tau_{\beta}$  at exactly  $\tau_o$ , the primitive relaxation time of the coupling model. The latter is calculated by Eq. (3) from the KWW parameters,  $\tau_{\alpha}$  and  $n$ , used to fit the  $\alpha$ -peak at any temperature. This constraint [i.e., Eq. (2)] imposed on  $\tau_{\beta}$  certainly somewhat compromises the quality of the fits that could be obtained with  $\tau_{\beta}$  floating. Nevertheless, good fits have been achieved, even with the constraint imposed, as can be judged by inspection of Fig. 2.

## B. Properties of the $\beta$ -relaxation

From the fits to the spectra in Figs. 1–3, we find the properties of the  $\alpha$ -relaxation and the  $\beta$ -relaxation in glycerol, PC and PG are in common. The dielectric strength  $\Delta\varepsilon_{\beta}$  of the  $\beta$ -relaxation increases with temperature, as suggested by the monotonic increase in height of the  $\beta$ -peak. On the other hand, the width of the  $\beta$ -peak narrows with increasing temperature. These properties are in accord with the properties of resolved  $\beta$ -peak in Class B glass-formers. In Figs. 4

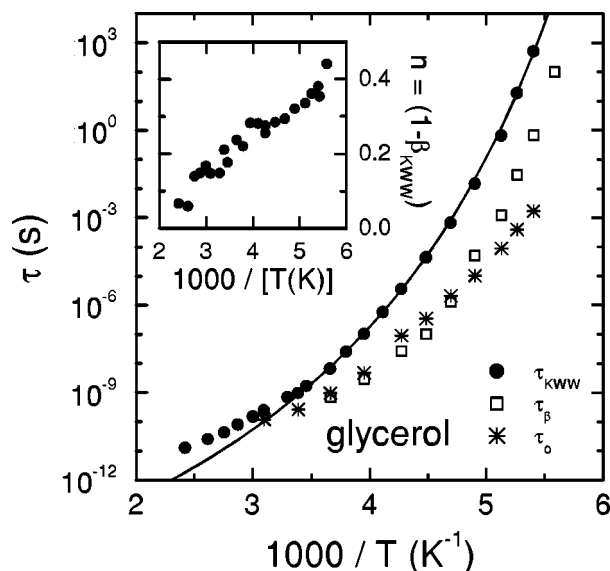


FIG. 4. Temperature dependences of the  $\alpha$ -relaxation time,  $\tau_\alpha$ , of the KWW function and the  $\beta$ -relaxation time,  $\tau_\beta$ , of glycerol used to fit the dielectric spectra in Fig. 1. The solid curve is the fit of the lower temperature values of  $\tau_\alpha$ , by a VFTH equation ( $\tau_\infty = 2.5 \times 10^{-16}$  s,  $D = 20.7$ ). Shown also are the primitive relaxation times,  $\tau_o$ , calculated at each temperature from the parameters of the KWW function used. Note the tendency of all three relaxation times to merge at the temperature,  $T_B$ , where the VFTH law no longer fits the data at higher temperatures. The inset shows the temperature dependence of the coupling parameter,  $n$ , or equivalently  $(1 - \beta_{\text{KWW}})$ , used in the KWW function to fit the dielectric dispersion in Fig. 1.

and 5, we plot  $\tau_\beta$  as a function of reciprocal temperature together with  $\tau_\alpha$  and  $\tau_o$  for glycerol and PG, respectively. The insets show the Kohlrausch-exponent in the form of  $n = 1 - \beta_{\text{KWW}}$ . From these plots, the temperature dependence of the  $\beta$ -relaxation in Class A glass-formers under the condition of thermodynamic equilibrium can be gleaned. First of all, the temperature dependence of  $\tau_\beta$  deviates from Arrhenius, although the deviation is much less than that of  $\tau_\alpha$  because the temperature dependence of  $\tau_\beta$  is significantly weaker than that of  $\tau_\alpha$  at low temperatures. This becomes especially evident for glycerol, where the data were taken to higher temperatures (frequencies) than in PG. Certainly, the parameters of the  $\beta$ -relaxation have relatively high uncertainties, due to the fact that, for the description of the excess wing, the right flank of the  $\beta$ -peak is mainly used. However, it is not possible to describe the experimental data, assuming a thermally activated behavior of  $\tau_\beta$  and the found non-Arrhenius behavior has a high significance because it is commonly believed that the J–G  $\beta$ -relaxation time has Arrhenius temperature dependence. This common belief comes from the Class B glass-formers, where the J–G relaxation is clearly resolved, particularly at temperatures below  $T_g$ , and indeed, it is Arrhenius. However, the J–G relaxation cannot be easily resolved at temperatures above  $T_g$ , even in Class B small molecular glass-formers, because it tends to merge with the  $\alpha$ -relaxation rather quickly as temperature is raised above  $T_g$ . Hence, there is little data on the J–G relaxation at temperatures above  $T_g$  in Class B glass-formers to verify whether the Arrhenius dependence below  $T_g$  will continue to hold above  $T_g$  or not. Our results of the J–G relaxation in glycerol, propylene carbonate and propylene glycol indicate

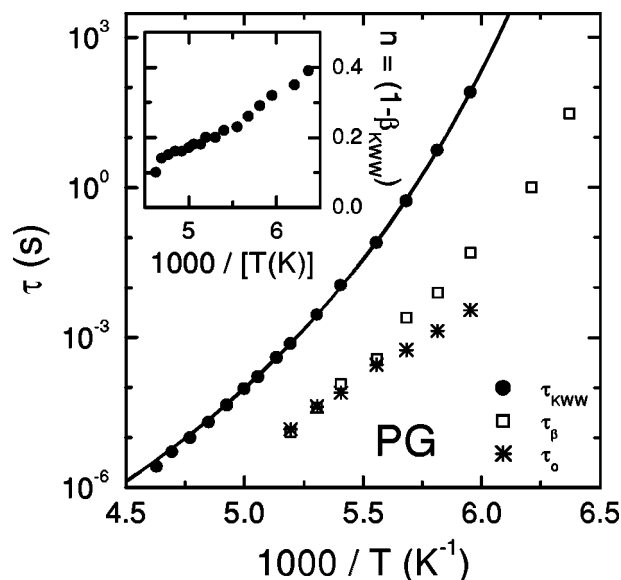


FIG. 5. Temperature dependences of the  $\alpha$ -relaxation time,  $\tau_\alpha$ , of the KWW function and the  $\beta$ -relaxation time,  $\tau_\beta$ , of propylene glycol (PG) used to fit the dielectric spectra in Fig. 3. The solid curve is the fit of the lower temperature values of  $\tau_\alpha$ , by a VFTH equation ( $\tau_\infty = 4.7 \times 10^{-13}$  s,  $D = 12.0$ ). Shown also are the primitive relaxation times,  $\tau_o$ , calculated at each temperature from the parameters of the KWW function used. The inset shows the temperature dependence of the coupling parameter,  $n = 1 - \beta_{\text{KWW}}$ , used in the KWW function to fit the dielectric dispersion in Fig. 3.

that  $\tau_\beta$  is non-Arrhenius. Similar conclusion was reached in the dielectric studies of primary<sup>44</sup> and secondary alcohols.<sup>45</sup>

The difference between  $\tau_\beta$  and  $\tau_\alpha$  monotonically decreases with increasing temperature. In glycerol, the two relaxation times tend to become quite close at temperatures higher than about 300 K. This temperature turns out to be the crossover temperature,  $T_B$ , found by Stickel *et al.*,<sup>46,47</sup> where his dielectric glycerol data of  $\tau_\alpha$  follow one Vogel–Fulcher–Tammann–Hesse (VFTH) equation,<sup>48</sup>  $\tau_\alpha = \tau_\infty \exp[DT_{\text{VF}}/(T - T_{\text{VF}})]$ , for  $T > T_B$  and another VFTH equation for  $T < T_B$ . Stickel arrived at the conclusion of a crossover by using his derivative analysis method<sup>47,49–51</sup> on isothermal data taken at many evenly spaced temperatures. As seen in Fig. 4, already without employing the derivative method, our own glycerol dielectric data of  $\tau_\alpha$  show a clear deviation from a low-temperature VFTH behavior above about 290 K ( $1000/T \approx 3.45 \text{ K}^{-1}$ ,  $\tau_\alpha > 10^9$  s). The calculation of derivatives leads to an increased scatter of the data points. To take advantage of the large database available for glycerol in literature, in Refs. 29 and 30, a polynomial fit to the  $\tau_\alpha$  data of six different publications, including the present data shown in Fig. 4, was applied. When subjected to the derivative analysis, these results also indicate that a single VFTH equation describes well the data in the low temperature region of  $T < 290$  K. Again, the derivative analysis in Refs. 29 and 30 admits another VFTH law to describe the temperature dependence of  $\tau_\alpha$  in the narrow region of  $3 < (1000/T) < 3.5 \text{ K}^{-1}$ , consistent with Stickel's conclusion. However at even higher temperatures,  $2.4 < (1000/T) < 3 \text{ K}^{-1}$ , the temperature dependence of  $\tau_\alpha$  becomes more complicated. Our glycerol data extend  $\tau_\alpha$  down to  $10^{-11}$  s, while that of Stickel are longer than  $10^{-10.5}$  s and, in addition, the higher

frequencies accessible to us, at elevated temperatures enable the observation of the high-frequency flank of the  $\alpha$ -peak up to higher frequencies. Therefore, possibly some inaccuracy of Stickel's measurements near the high frequency limit of his experimental window is the cause of the discrepancy between the results of the derivative analysis of Stickel and that in Refs. 29 and 30. Nevertheless, our data of  $\tau_\alpha$ , as well as Stickel's, clearly show a deviation of the VFT law at temperatures above approximately 300 K, and this is the temperature at which the three relaxation times,  $\tau_\alpha$ ,  $\tau_\beta$  and  $\tau_o$ , collapse to nearly the same value.

In Class B glass-formers, including ortho-terphenyl (OTP)<sup>52</sup> and bis-methoxy-phenyl-cyclohexane (BMPC),<sup>47</sup> evidence for the existence of  $T_B$  is even clearer than in the case of glycerol. In these Class B glass-formers,  $\tau_\beta$  of the J-G  $\beta$ -relaxation that can be clearly resolved, has an Arrhenius temperature dependence at temperatures near and below  $T_g$ . When such Arrhenius temperature dependence is extrapolated to temperatures above  $T_g$ , it intersects the curve of  $\tau_\alpha$  at a temperature  $T_\beta$ , which is very close to  $T_B$ . This apparent intersection is often considered as tendency of the merging of the  $\alpha$ - and the  $\beta$ -relaxation at  $T_\beta \approx T_B$ . The Arrhenius extrapolation of the actual  $\tau_\beta(T)$  data near and above  $T_g$  that is needed for  $\tau_\beta$  to reach the intersection with  $\tau_\alpha$  at  $T_\beta$ , covers about merely one decade of frequency for OTP and BMPC. Therefore, if the actual temperature dependence of  $\tau_\beta$  of Class B glass-formers above  $T_g$  were not Arrhenius, the possible intersection of  $\tau_\beta$  and  $\tau_\alpha$  would occur at a temperature different from  $T_\beta$ . However, we can expect that this difference is small because of the short extrapolation either in temperature or frequency needed by the supposedly Arrhenius  $\tau_\beta$  to merge with  $\tau_\alpha$  in Class B glass-formers.

Let us now compare this property of Class B glass-formers with that of glycerol. It is clear from Fig. 4 that the tendency of the  $\alpha$ - and the  $\beta$ -relaxation to merge at a temperature near  $T_B$  seems to happen also in glycerol, a Class A glass-former. Thus, Class A and Class B glass-formers seem to behave in the same manner, at least as far as the existence of the J-G  $\beta$ -relaxation and the tendency of the  $\alpha$ - and the  $\beta$ -relaxation to nearly merge at  $T \approx T_B$  are concerned. The only difference is in the degree of separation between the  $\alpha$ - and the  $\beta$ -relaxation at  $T_g$ , measured by the difference,  $[\log \tau_\alpha(T_g) - \log \tau_\beta(T_g)]$ . Class B glass-formers have larger  $[\log \tau_\alpha(T_g) - \log \tau_\beta(T_g)]$  than Class A glass-formers. Therefore the use of the terms Class A and Class B for glass-formers turns out to be unnecessary because their difference is only in the degree of separation between the  $\alpha$ - and the  $\beta$ -relaxation frequencies.

In Figs. 4 and 5, the stars denote the primitive relaxation time,  $\tau_o$ , calculated from the parameters of the  $\alpha$ -relaxation using Eq. (3). In both glycerol and PG,  $\tau_\beta$  and  $\tau_o$  are nearly the same at all temperatures except near and below  $T_g$ . However, the difference between  $\tau_\beta$  and  $\tau_o$  at the low temperatures may be less significant than as it appears in Figs. 4 and 5. The reason is that, at low temperatures, the  $\beta$ -relaxation peak becomes very broad (see Figs. 1–3) and the uncertainty in the most probable  $\tau_\beta$  is hence large.

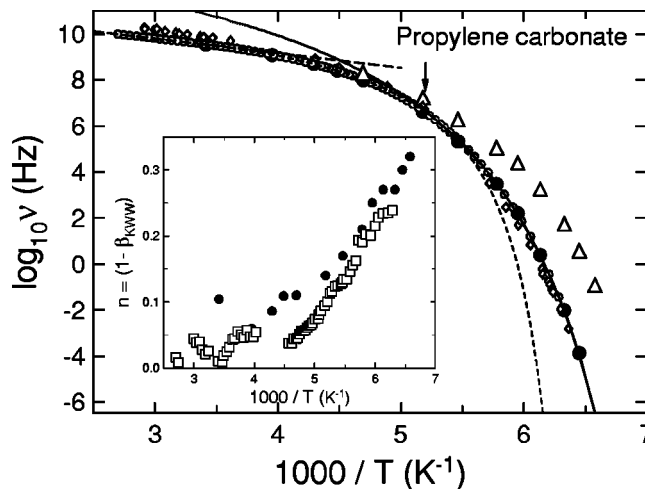


FIG. 6. Temperature dependences of the propylene carbonate  $\alpha$ -relaxation peak frequency (filled circles) and the  $\beta$ -relaxation peak frequency (open triangles) from the Cole-Cole curves in Fig. 2. Shown also are the  $\alpha$ -relaxation peak frequency (open circles) from the dielectric data of Stickel (Refs. 47,50). The open diamonds are logarithm of the reciprocal of the viscosity data (Refs. 47,50) shifted by a constant to match the dielectric data. The solid and dashed lines are respectively the VFT law for the  $\alpha$ -relaxation peak frequency for the lower temperature regime ( $T < 192$  K) and for the intermediate higher temperature regime of ( $192 K < T < 265$  K). The dashed straight line is the Arrhenius fit to the high temperature data of Stickel given by him. The inset shows the temperature dependence of the coupling parameter,  $n$ , or equivalently  $(1 - \beta_{KWW})$ , used in the KWW function to fit the dielectric dispersion in Fig. 2 (filled circles). The open squares are  $(1 - \beta_{KWW})$  calculated from  $w$ , the full widths at half maximum of the dielectric loss peak normalized to that of an ideal Debye loss peak, given by Stickel by using the equation,  $n \equiv 1 - \beta_{KWW} = 1.047(1 - w^{-1})$ , from Dixon (Ref. 53).

Within this large uncertainty,  $\tau_\beta$  can be considered to be nearly the same  $\tau_o$  at the lower temperatures.

In Figs. 1 and 3, for 185 K and 168 K, respectively, we also show a fit curve calculated with  $\tau_\beta$  fixed at  $\tau_o$  (dashed-dotted line). The agreement with the experimental data in the transition region between  $\alpha$ -peak and excess wing is somewhat worse than that achieved with the free fits. However, this disagreement certainly is not too severe and may be even further reduced by making adjustments to the parameters pertaining to the  $\alpha$ -peak [which by means of Eq. (3) changes again  $\tau_o$ ]. Thus, for all intents and purposes, the experimental data in glycerol and PG are consistent with the assumption that  $\tau_\beta$  is equal or nearly equal to  $\tau_o$ .

Further support to this notion is provided by the fits to the dispersion of PC (Fig. 2) that have constrained  $\tau_\beta$  to be exactly equal to  $\tau_o$ . Naturally, these good fits to PC provide evidence for near coincidence of  $\tau_\beta$  and  $\tau_o$  in Class A glass-formers in the equilibrium liquid state. In Fig. 6, we plotted the logarithm of the  $\alpha$ -peak frequency  $\nu_\alpha$  (filled circles) obtained from the fits to our PC data (Fig. 2) and the  $\beta$ -peak frequency  $\nu_\beta = 1/(2\pi\tau_o)$  (open triangles) used for the fits. The open circles are  $\log \nu_\alpha$  and the open diamonds are  $\log(c\eta^{-1})$  given by Stickel *et al.*,<sup>47,50</sup> where  $c$  is a constant and  $\eta$  the shear viscosity. There is overall good agreement between our data and that of Stickel *et al.* The relaxation times,  $\tau_\alpha$  and  $\tau_\beta \equiv \tau_o$ , are given with high accuracy here for PC by  $\tau_\alpha = (2\pi\nu_\alpha)^{-1}$  and  $\tau_\beta = (2\pi\nu_\beta)^{-1}$ , respectively. The coupling parameter,  $n(T) \equiv [1 - \beta_{KWW}(T)]$ , used to calcu-

late  $\tau_o$  by Eq. (3) from  $\tau_\alpha(T)$  is shown in the inset. The filled circles are from the present work with  $\beta_{\text{KWW}}(T)$  being the exponent of the KWW function that is employed to fit the  $\varepsilon''(\nu)$  data in Fig. 2. The open squares are  $(1 - \beta_{\text{KWW}})$  calculated from  $w$ , the full widths at half maximum of the dielectric loss peak normalized to that of an ideal Debye loss peak, given by Stickel<sup>47</sup> by using the equation,  $n \equiv 1 - \beta_{\text{KWW}} = 1.047(1 - w^{-1})$ , from Dixon.<sup>53</sup> The non-Arrhenius temperature dependence of  $\tau_\beta$ , and its tendency to merge with  $\tau_\alpha$ , is even clearer in PC than in glycerol (Fig. 4). Stickel has shown by the derivative analysis of his dielectric PC data taken over many finely spaced temperatures (open circles in Fig. 6) that the temperature dependence of the  $\alpha$ -peak frequency,  $\nu_\alpha(T)$ , can be described by one VFTH law for  $T < T_B$  (solid line) and a different VFTH law for  $265 \text{ K} > T > T_B$  (dashed line) with  $T_B \approx 192 \text{ K}$  (located by the vertical arrow in Fig. 6) and  $\nu_\alpha(T_B) \approx 10^7 \text{ Hz}$ . The derivative analysis, performed in Refs. 29 and 30 on combined data from nine different sources, including the present data and those of Stickel *et al.*, does show a somewhat smoother crossover with no clearly defined VFTH regions. As remarked before, this discrepancy with Stickel's analysis is not too severe because already, without employing the derivative analysis, a deviation from a low-temperature VFTH behavior can be observed. The exact onset temperature of this deviation to some extent depends on the temperature range of the data used to determine the VFTH parameters. Stickel's VFTH curves indicate that it occurs near 200 K (Fig. 6). But in Ref. 18 it was reported to occur at 230 K. Both temperatures are very close to the temperatures where the  $\beta$ -peak and the  $\alpha$ -peak tend to merge in Fig. 6 and the merging seems to be nearly complete at higher temperatures. It is also interesting to observe from the inset of Fig. 6 that  $n = (1 - \beta_{\text{KWW}})$  decreases with increasing temperature and becomes small (about 0.1 or less) when  $T > T_B$ . The small discrepancy of  $n$ ,<sup>54</sup> reported by Stickel and in other publications from the same group,<sup>55</sup> and  $n$  obtained from our data was discussed in Refs. 29 and 30. It is not of relevance for the following discussion; the only important point is the fact that  $n$  strongly decreases with increasing temperature, and above about 200 K it reaches a low value,  $n \approx 0.1$ . In glycerol and PG (for both  $T_B \approx 300 \text{ K}$ )<sup>47</sup> the situation is similar, with  $n \approx 0.15$  for  $T > 300 \text{ K}$  in glycerol and  $n$  of PG also approaching comparable small values at high enough temperature (inset of Figs. 4 and 5).

The quantity,  $n \equiv (1 - \beta_{\text{KWW}})$ , is a measure of the departure of the  $\alpha$ -relaxation from linear exponential decay for an independent relaxation process. It is interpreted in the coupling model as the degree of intermolecular cooperativity or coupling of the  $\alpha$ -relaxation. The fact that it becomes small when  $T > T_B$ , signals the drastic reduction of intermolecular cooperativity of the  $\alpha$ -relaxation in this high temperature regime. Once intermolecular cooperativity is removed from the  $\alpha$ -relaxation, it becomes the same as the primitive relaxation in the coupling model and resembles the  $\beta$ -relaxation, which is also devoid of intermolecular cooperativity. Therefore, the merging of the  $\alpha$ -relaxation and  $\beta$ -relaxation in Fig. 6 can be understood as a natural consequence of the temperature dependence of  $n \equiv (1 - \beta_{\text{KWW}})$ . A similar situation holds also

for OTP.<sup>13,56</sup> Again, at temperatures higher than  $T_\beta \approx T_g$ ,  $n \equiv (1 - \beta_{\text{KWW}})$  of OTP becomes small, and all relaxation times,  $\tau_\alpha$ ,  $\tau_o$  and  $\tau_\beta$ , are approximately equal. The proximity of  $\tau_\beta$  and  $\tau_o$  in Class A glass-formers is also found in OTP<sup>56</sup> and in poly(vinyl acetate), both Class B glass-former<sup>57</sup> and in an orientational glass.<sup>13</sup> Hence, this property of the  $\beta$ -relaxation is common to both classes of glass-formers.

By inspection of the Cole–Cole curves that model the  $\beta$ -relaxation of glycerol, PC, and PG in Figs. 1, 2 and 3, respectively, we can see that the width decreases but the height increases with increasing temperature. These trends of the J–G  $\beta$ -peak in the Class A glass-formers are the same as that shown by the  $\beta$ -relaxation in Class B glass-formers such as toluene,<sup>58</sup> 3-fluoranioline,<sup>58</sup> sorbitol,<sup>59</sup> and polybutadiene,<sup>60</sup> and can be considered as additional evidence that the  $\beta$ -relaxation of glycerol, PC, and PG we have resolved from their dielectric spectra are indeed the J–G  $\beta$ -relaxation. Thus the results of this work confirms the belief<sup>7,8</sup> that the J–G relaxation is an intrinsic feature of the glass transition of all glass-formers. Only its relaxation strength and the separation between its relaxation time and the  $\alpha$ -relaxation time may vary from one glass-former to another. Hence, as far as the existence of the J–G relaxation is concerned, there is no need to classify glass-formers into Class A and Class B anymore. Being a ubiquitous property of glass transition, the mechanism behind the J–G relaxation is certainly of great interest. There has been suggestion by Johari that the J–G relaxation arises from hindered rotation of some molecules in some distribution of local regions (islands of mobility). The hindered rotation is an isolated event and is to be distinguished from the cooperative motion of a larger number of molecules involved in the  $\alpha$ -relaxation. This suggestion is appealing particularly in the glassy state where frozen density fluctuations persist. At temperatures above  $T_g$ , the results obtained on the J–G relaxation in this work suggest a slightly different variation of the mechanism as follows. In as much as the  $\alpha$ -relaxation requires a cooperative motion of a number of molecules, there are also molecules that statistically happen to not be needed to participate in any of the slower cooperative motions. A crude way to visualize this possibility is to partition space into a collection of cooperative rearranging regions (CRR).<sup>61</sup> Unless in the ideal case that the latter completely fills the entire space, there will be molecules left over in the “boundary” regions that are free to execute isolated hindered rotational motion in a local environment, which is the J–G relaxation. Since at temperatures above  $T_g$  the liquid is in equilibrium, the boundary molecules appear throughout the liquid in a statistical sense. As temperature increases above  $T_g$ , the size of the CRR decreases. It follows from this mechanism for the J–G relaxation that the number of molecules executing the J–G relaxation will increase with increasing temperature because of a concomitant decrease in the size of the CRR. It follows that the relaxation strength of the J–G relaxation will increase with temperature as observed in our data above  $T_g$ . A smaller size of the CRR will reduce the fluctuation of the local environment of the molecules executing the J–G relaxation for two reasons. First,

just from geometric consideration, the smaller size of the CRR naturally causes less fluctuation of the local environment. Second, smaller CRR drastically reduce  $\tau_\alpha^{61}$  and hence the difference between  $\tau_\alpha$  and the faster J–G relaxation time. Therefore, the loss spectrum of the J–G relaxation will become narrower with increasing temperature, consistent with the trend seen in Figs. 1–3. In the high temperature limit when the size of CRR approaches unity, there is vanishing distinction between the molecules involved in the  $\alpha$ -relaxation and the J–G relaxation and that is the reason why they tend to merge together to form a narrow peak in the loss spectrum (see Figs. 1–3). In Johari's original model and this slightly modified model, the J–G relaxation is a free relaxation in local environments, and there is absence of cooperativity. It is not surprising that its relaxation time  $\tau_\beta$  is not much different from the primitive relaxation time  $\tau_o$  of the coupling model because the latter is also a molecular relaxation time that is devoid of cooperativity with other molecules.

#### IV. CONCLUSION

From analyses of the dielectric relaxation data of glycerol, propylene carbonate and propylene glycol, reinforced by the results upon aging in all these three Class A glass-formers, we can conclude that the J–G  $\beta$ -relaxation also does exist in Class A glass-formers in the equilibrium liquid state. The properties of the  $\beta$ -relaxation in Class A glass-formers in the equilibrium liquid state include:

- (i) The temperature dependence of the  $\beta$ -relaxation time  $\tau_\beta(T)$  is non-Arrhenius but weaker than that of the  $\alpha$ -relaxation time  $\tau_\alpha(T)$ .
- (ii) The tendency of the  $\alpha$ - and the  $\beta$ -relaxation to merge at some temperature  $T_\beta$ , which is near  $T_B$ . Here  $T_B$  is the temperature above which the VFTH law that fits well the  $\tau_\alpha(T)$  data for  $T < T_B$  no longer works.
- (iii) As temperature is decreased, the  $\beta$ -relaxation peak broadens dramatically and its height or relaxation strength decreases. The  $\beta$ -relaxation peak becomes very broad and the maximum loss falls to very low values at temperatures near or below  $T_g$ . The excess wing in the dielectric loss spectrum is the high frequency flank of the broad  $\beta$ -relaxation peak submerged under the much more intense  $\alpha$ -peak.
- (iv) At temperatures above  $T_g$ ,  $\tau_\beta(T)$  and the primitive relaxation time,  $\tau_o(T)$ , of the coupling model are approximately equal in order of magnitude.
- (v) The KWW exponent of the  $\alpha$ -relaxation increases monotonically with increasing temperature. At temperatures above  $T_\beta$  or  $T_B$ , the KWW exponent has increased already to values close to unity, indicating that the  $\alpha$ -relaxation has become nearly Debye-like, although the exact Debye limit may not be realized within the temperature range of measurements.

Some of the properties (i)–(iv) can be understood from the precept and prediction of the coupling model.

#### ACKNOWLEDGMENTS

This work was supported by the Deutsche Forschungsgemeinschaft, Grant No. LO264/8-1 and partly by the BMBF, contract No. 13N6917. The part of the work performed at the Naval Research Laboratory was supported by the Office of Naval Research.

- <sup>1</sup>P. K. Dixon, L. Wu, S. R. Nagel, B. D. Williams, and J. P. Carini, *Phys. Rev. Lett.* **65**, 1108 (1990).
- <sup>2</sup>A. Hofmann, F. Kremer, E. W. Fischer, and A. Schönhal, in *Disorder Effects on Relaxational Processes*, edited by R. Richert and A. Blumen (Springer, Berlin, 1994), p. 309.
- <sup>3</sup>R. L. Leheny and S. R. Nagel, *Europhys. Lett.* **39**, 447 (1997).
- <sup>4</sup>A. Kudlik, S. Benkhof, T. Blochowicz, C. Tschirwitz, and E. Rössler, *J. Mol. Struct.* **479**, 201 (1999).
- <sup>5</sup>R. V. Chamberlin, *Phys. Rev. B* **48**, 15638 (1993).
- <sup>6</sup>G. Tarjus and D. Kivelson, in *Supercooled Liquids: Advances and Novel Applications*, edited by J. T. Fourkas et al. (American Chemical Society, Washington, D.C., 1997), p. 67.
- <sup>7</sup>G. P. Johari and M. Goldstein, *J. Chem. Phys.* **53**, 2372 (1970).
- <sup>8</sup>G. P. Johari, in *The Glass Transition and the Nature of the Glassy State*, edited by M. Goldstein and R. Simha [*Ann. N.Y. Acad. Sci.* **279**, 117 (1976)].
- <sup>9</sup>J. Wiedersich, T. Blochowicz, S. Benkhof, A. Kudlik, N. V. Surovtsev, C. Tschirwitz, V. N. Novikov, and E. Rössler, *J. Phys.: Condens. Matter* **11**, A147 (1999).
- <sup>10</sup>In fact, in Refs. 4 and 9 the terms "Type A" and "Type B" were used. However, these terms were earlier introduced in the discussion of dielectric properties of polymers [W. H. Stockmayer, *Pure Appl. Chem.* **15**, 539 (1987)]. Therefore, to avoid confusion, in the present work we use the terms "Class A" and "Class B" instead.
- <sup>11</sup>N. B. Olsen, *J. Non-Cryst. Solids* **235–237**, 399 (1998).
- <sup>12</sup>M. Jiménez-Ruiz, M. A. González, F. J. Bermejo, M. A. Miller, N. O. Birge, I. Cendoya, and A. Alegria, *Phys. Rev. B* **59**, 9155 (1999).
- <sup>13</sup>C. León and K. L. Ngai, *J. Phys. Chem. B* **103**, 4045 (1999).
- <sup>14</sup>C. León, K. L. Ngai, and C. M. Roland, *J. Chem. Phys.* **110**, 11585 (1999).
- <sup>15</sup>H. Wagner and R. Richert, *J. Chem. Phys.* **110**, 11660 (1999).
- <sup>16</sup>U. Schneider, R. Brand, P. Lunkenheimer, and A. Loidl, *Phys. Rev. Lett.* **84**, 5560 (2000).
- <sup>17</sup>U. Schneider, P. Lunkenheimer, R. Brand, and A. Loidl, *J. Non-Cryst. Solids* **235–237**, 173 (1998).
- <sup>18</sup>U. Schneider, P. Lunkenheimer, R. Brand, and A. Loidl, *Phys. Rev. E* **59**, 6924 (1999).
- <sup>19</sup>A. Kudlik, S. Benkhof, R. Lenk, and E. Rössler, *Europhys. Lett.* **32**, 511 (1995).
- <sup>20</sup>S. H. Chung, G. P. Johari, and K. Pathmanathan, *J. Polym. Sci., Part B: Polym. Phys.* **24**, 2655 (1986).
- <sup>21</sup>R. L. Leheny and S. R. Nagel, *Phys. Rev. B* **57**, 5154 (1998).
- <sup>22</sup>G. P. Johari and E. Whalley, *Faraday Symp. Chem. Soc.* **6**, 23 (1972); G. P. Johari and K. Pathmanathan, *J. Chem. Phys.* **85**, 6811 (1986).
- <sup>23</sup>H. Fujimori and M. Oguni, *J. Chem. Thermodyn.* **26**, 367 (1994); W. Schnauss, F. Fajara, and H. Sillescu, *J. Chem. Phys.* **97**, 1378 (1992).
- <sup>24</sup>K. L. Ngai, *Phys. Rev. E* **57**, 7346 (1998); *J. Chem. Phys.* **109**, 6982 (1998).
- <sup>25</sup>R. Kohlrausch, *Ann. Phys. (Leipzig)* **167**, 56 (1854); *ibid.* **167**, 179 (1854); G. Williams and D. C. Watts, *Trans. Faraday Soc.* **66**, 80 (1970).
- <sup>26</sup>K. L. Ngai, *Comments Solid State Phys.* **9**, 127 (1979).
- <sup>27</sup>K. Y. Tsang and K. L. Ngai, *Phys. Rev. E* **54**, 3067 (1997); K. Y. Tsang and K. L. Ngai, *Phys. Rev. E* **56**, R17 (1997); K. L. Ngai and K. Y. Tsang, *Phys. Rev. E* **60**, 4511 (1999).
- <sup>28</sup>K. L. Ngai and R. W. Rendell, *Supercooled Liquids, Advances and Novel Applications*, ACS Symposium Series Vol. 676, edited by J. T. Fourkas, D. Kivelson, U. Mohanty, and K. Nelson (American Chemical Society, Washington, D.C., 1997), Chap. 4, pp. 45–66.
- <sup>29</sup>P. Lunkenheimer, U. Schneider, R. Brand, and A. Loidl, *Contemp. Phys.* **41**, 15 (2000).
- <sup>30</sup>P. Lunkenheimer, *Dielectric Spectroscopy of Glassy Dynamics* (Shaker, Aachen, 1999).
- <sup>31</sup>U. Schneider, P. Lunkenheimer, A. Pimenov, R. Brand, and A. Loidl, *Ferroelectrics*, cond-mat/9908279 (in press).

- <sup>32</sup>P. Lunkenheimer, U. Schneider, R. Brand, and A. Loidl, *Physikalische Blätter* **56**, 35 (2000).
- <sup>33</sup>P. Lunkenheimer, A. Pimenov, M. Dressel, Yu. G. Goncharov, R. Böhmer, and A. Loidl, *Phys. Rev. Lett.* **77**, 318 (1996); P. Lunkenheimer, A. Pimenov, M. Dressel, B. Gorshunov, U. Schneider, B. Schiener, and A. Loidl, in *Supercooled Liquids, Advances and Novel Applications*, edited by J. T. Fourkas *et al.*, ACS Symposium Series Vol. 676 (American Chemical Society, Washington, D.C., 1997), p. 168.
- <sup>34</sup>J. Wuttke, M. Ohl, M. Goldammer *et al.*, *Phys. Rev. E* **61**, 2730 (2000); W. Götze and Th. Voigtmann, *Phys. Rev. E* **61**, 4133 (2000).
- <sup>35</sup>P. Lunkenheimer, U. Schneider, R. Brand, and A. Loidl, in *Slow Dynamics in Complex Systems: Eighth Tohwa University International Symposium*, edited by M. Tokuyama and I. Oppenheim (AIP, New York, 1999), AIP Conf. Proc. No. 469, p. 433; R. Casalini, K. L. Ngai, and C. M. Roland, *J. Chem. Phys.* **112**, 5181 (2000).
- <sup>36</sup>For the concept of the fictive temperature, see e.g., C. T. Moynihan *et al.*, *Ann. N.Y. Acad. Sci.* **279**, 15 (1976).
- <sup>37</sup>U. Schneider *et al.* (unpublished).
- <sup>38</sup>R. V. Chamberlin, *Phys. Rev. Lett.* **82**, 2520 (1999).
- <sup>39</sup>For a review of various theories of the glass transition, see: J. Jäckle, *Rep. Prog. Phys.* **49**, 171 (1986).
- <sup>40</sup>D. W. Davidson and R. H. Cole, *J. Chem. Phys.* **18**, 1417 (1950); D. W. Davidson and R. H. Cole, *J. Chem. Phys.* **19**, 1484 (1951).
- <sup>41</sup>K. S. Cole and R. H. Cole, *J. Chem. Phys.* **9**, 341 (1941).
- <sup>42</sup>At low temperatures, the transition region between  $\alpha$ -peak and excess wing seems slightly too smooth to be met perfectly by the fit curves. As was shown in Refs. 16 and 30, this problem can be overcome using a CD function for the  $\alpha$ -peak.
- <sup>43</sup>U. Bengtzelius, W. Götze, and A. Sjölander, *J. Phys. C* **17**, 5915 (1984); E. Leutheuser, *Phys. Rev. A* **29**, 2765 (1984); W. Götze, *Z. Phys. B: Condens. Matter* **60**, 195 (1985); W. Götze and L. Sjögren, *Rep. Prog. Phys.* **55**, 241 (1992).
- <sup>44</sup>R. Brand, P. Lunkenheimer, U. Schneider, and A. Loidl, *Phys. Rev. B* **62**, 8878 (2000).
- <sup>45</sup>O. E. Kalinovskaya and J. K. Vij, *J. Chem. Phys.* **112**, 3262 (2000).
- <sup>46</sup>F. Stickel, E. W. Fischer, A. Schönhals, and F. Kremer, *Phys. Rev. Lett.* **73**, 2936 (1994).
- <sup>47</sup>F. Stickel, *Untersuchung der Dynamik in niedermolekularen Flüssigkeiten mit Dielektrischer Spektroskopie* (Shaker, Aachen, 1995).
- <sup>48</sup>H. Vogel, *Z. Phys.* **22**, 645 (1921); G. S. Fulcher, *J. Am. Ceram. Soc.* **8**, 339 (1925); G. Tammann and W. Hesse, *Z. Anorg. Allg. Chem.* **156**, 245 (1926).
- <sup>49</sup>F. Stickel, E. W. Fischer, and R. Richert, *J. Chem. Phys.* **102**, 6251 (1995).
- <sup>50</sup>F. Stickel, E. W. Fischer, and R. Richert, *J. Chem. Phys.* **104**, 2043 (1996).
- <sup>51</sup>K. L. Ngai, J. H. Magill, and D. J. Plazek, *J. Chem. Phys.* **112**, 1887 (2000).
- <sup>52</sup>C. Hansen, F. Stickel, T. Berger, R. Richert, and E. W. Richert, *J. Chem. Phys.* **107**, 1086 (1997).
- <sup>53</sup>P. K. Dixon, *Phys. Rev. B* **42**, 8179 (1990).
- <sup>54</sup>In fact, in Refs. 29 and 30, instead of  $n = 1 - \beta_{\text{KWW}}$ , the exponent of the CD function  $\beta_{\text{CD}}$  was discussed, which is closely related to  $\beta_{\text{KWW}}$ .
- <sup>55</sup>A. Schönhals, F. Kremer, A. Hofmann, E. W. Fischer, and E. Schlosser, *Phys. Rev. Lett.* **70**, 3459 (1993).
- <sup>56</sup>K. L. Ngai, *J. Phys.: Condens. Matter* **11**, A119 (1999).
- <sup>57</sup>K. L. Ngai and C. M. Roland, *Polymer* (in press).
- <sup>58</sup>J. Wierdersich, T. Blochowicz, S. Benkhof, A. Kudlik, N. V. Surovtsev, C. Tschirwitz, V. N. Novikov, and E. Rössler, *J. Phys.: Condens. Matter* **11**, A147 (1999).
- <sup>59</sup>R. Nozaki, D. Suzuki, S. Ozawa, and Y. Shiozaki, *J. Non-Cryst. Solids* **235–237**, 393 (1998).
- <sup>60</sup>N. G. McCrum, B. E. Read, and G. Williams, *Anelastic and Dielectric Effects in Polymeric Solids* (Wiley, London, 1967 and Dover Publications, New York, 1991); A. Hofmann, A. Alegria, J. Colmenero, L. Willner, E. Buscaglia, and N. Hadjichristidis, *Macromolecules* **29**, 129 (1996).
- <sup>61</sup>G. Adam and J. H. Gibbs, *J. Chem. Phys.* **43**, 139 (1965).